RANK ligand inhibition plus docetaxel improves survival and reduces tumor burden in a murine model of prostate cancer bone metastasis

Robert E. Miller,[1] Martine Roudier,[2] Jon Jones,[1] Allison Armstrong,[1] Jude Canon,[3] and William C. Dougall[1]

Departments of [1]Hematology/Oncology Research and [2]Pathology, Amgen Washington, Seattle, Washington; and [3]Department of Hematology/Oncology Research, Amgen, Inc., Thousand Oaks, California

Abstract

Tumor cells induce excessive osteoclastogenesis, mediating pathologic bone resorption and subsequent release of growth factors and calcium from bone matrix, resulting in a ''vicious cycle'' of bone breakdown and tumor proliferation. RANK ligand (RANKL) is an essential mediator of osteoclast formation, function, and survival. In metastatic prostate cancer models, RANKL inhibition directly prevents osteolysis via blockade of osteoclastogenesis and indirectly reduces progression of skeletal tumor burden by reducing local growth factor and calcium concentrations. Docetaxel, a well-established chemotherapy for metastatic hormone-refractory prostate cancer, arrests the cell cycle and induces apoptosis of tumor cells. Suppression of osteoclastogenesis through RANKL inhibition may enhance the effects of docetaxel on skeletal tumors. We evaluated the combination of the RANKL inhibitor osteoprotegerin-Fc (OPG-Fc) with docetaxel in a murine model of prostate cancer bone metastasis. Tumor progression, tumor area, and tumor proliferation and apoptosis were assessed. OPG-Fc alone reduced bone resorption ($P < 0.001$ versus PBS), inhibited progression of established osteolytic lesions, and reduced tumor area ($P < 0.0001$ versus PBS). Docetaxel alone reduced tumor burden ($P < 0.0001$ versus PBS) and delayed the development of osteolytic lesions. OPG-Fc in combination with docetaxel suppressed skeletal tumor burden ($P = 0.0005$) and increased median survival time by 16.7% ($P = 0.0385$) compared with docetaxel alone. RANKL inhibition may enhance docetaxel effects by increasing tumor cell apoptosis as evident by increased active caspase-3. These studies show that inhibition of RANKL provides an additive benefit to docetaxel treatment in a murine model of prostate cancer bone metastasis and supports clinical evaluation of this treatment option in patients. [Mol Cancer Ther 2008;7(7):2160–9]

Introduction

Bone metastases are a frequent complication of cancer, occurring in up to 90% of cases of advanced prostate cancer, and essentially all terminal prostate cancer patients have bone metastases (1–3). The extent of skeletal disease in androgen-independent prostate cancer patients is prognostic for patient survival (4) and also contributes to skeletal complications, termed skeletal-related events, which include pathologic skeletal fractures, spinal cord compression, and a requirement for radiation therapy, or surgery to bone (2).

Radiographically, most prostate cancer bone metastases are classified as osteoblastic as opposed to other solid tumor metastases (e.g., breast and lung), which are typically osteolytic or mixed osteolytic/osteoblastic in nature (5). The characterization of bone metastases as either osteoblastic or osteolytic actually represents two extremes of a spectrum of dysregulated bone remodeling (6–9). Bone morphologic analyses have suggested that some primarily osteoblastic prostate tumors actually have a prominent lytic component (10). The concept that osteoclast activation accompanies all bone metastases, irrespective of radiographic diagnosis, is further supported by the finding that biochemical markers of bone resorption, in particular *N*-telopeptide type I collagen, are increased in bone metastases regardless of whether they are lytic, blastic, or mixed (11). Recently, a correlation between *N*-telopeptide type I collagen and clinical outcome, including skeletal-related events and survival, has been observed in patients with prostate cancer, breast cancer, and other solid tumors (e.g., non-small cell lung carcinoma, renal carcinoma, small-cell lung carcinoma, and thyroid carcinoma) and in patients with multiple myeloma (7, 12). Taken together, these findings suggest that the risk of skeletal complications and clinical outcome in metastatic bone disease are dependent in part on the capacity to control the level of osteoclast activity and the subsequent osteolysis.

Tumor cells interact with the bone microenvironment to induce osteoclastogenesis leading to the resultant bone destruction. Receptor activator of nuclear factor-κB ligand [RANK ligand (RANKL)] is a tumor necrosis factor ligand superfamily member that is essential for osteoclast formation, function, and survival (13). The critical role of RANKL

Received 1/14/08; revised 4/16/08; accepted 5/18/08.

Grant support: Amgen.

The costs of publication of this article were defrayed in part by the payment of page charges. This article must therefore be hereby marked *advertisement* in accordance with 18 U.S.C. Section 1734 solely to indicate this fact.

Requests for reprints: William C. Dougall, Department of Pathology, Amgen Washington, 1201 Amgen Court West, Seattle, WA 98119-3105. Phone: 206-265-7553; Fax: 206-217-0494.
E-mail: dougallw@amgen.com

doi:10.1158/1535-7163.MCT-08-0046

in cancer-induced bone disease has been seen in animal models of breast and prostate cancer bone metastases in which pharmacologic blockade of RANKL inhibited tumor-induced osteolysis and reduced the progression of skeletal tumor burden (14–16), suggesting that tumor-induced osteolysis ultimately depends on RANKL action. Because the osteolysis of bone matrix releases many growth factors and calcium that can promote tumor growth and survival (17), the reduction in skeletal tumor burden observed after RANKL inhibition can be explained, in part, by inhibition of tumor-induced osteoclast action.

Although advanced androgen-independent prostate cancer metastatic to bone is an incurable disease even after radiotherapy and chemotherapy (18), the chemotherapeutic agent docetaxel has been shown to increase survival, reduce pain, and improve health-related quality of life in patients with advanced prostate cancer (19, 20). However, despite the improvement in overall survival, nearly all patients in these clinical trials still progressed (19, 20). By targeting the bone microenvironment and reducing tumor-induced bone resorption with a RANKL inhibitor, tumor cells may become sensitized to the effects of chemotherapy. Here, we examined the *in vivo* effects of the RANKL inhibitor, osteoprotegerin-Fc (OPG-Fc), in combination with docetaxel on tumor-induced osteolysis, tumor burden, and survival in a mouse model of prostate cancer bone metastasis.

Materials and Methods

Tumor Cell Lines

The human prostate cancer cell line PC-3 was obtained from the American Type Culture Collection and cultured in RPMI supplemented with 10% fetal bovine serum, nonessential amino acids, sodium pyruvate, and glutamine. The PC-3 cells were adapted for growth in bone by two successive passages *in vivo* via intratibial injections. These cells were stably transduced to express firefly luciferase (Luc) for *in vivo* bioluminescent imaging (BLI) according to the following protocol.

Briefly, 1×10^5 PC-3 cells per well were seeded overnight in 12-well plates. The pLV411G-FLuc construct uses the murine EF1α promoter to express the enhanced firefly Luc reporter gene (Promega) upstream of EMCV-IRES green fluorescent protein (Diversa). PC-3 cells were transduced with specific lentiviral vectors by incubating 1×10^6 cells with 1×10^7 transducing units of vector in a single well of a 12-well tissue culture dish for 6 h in 500 μL RPMI containing 10 μg/mL DEAE-dextran. Green fluorescent protein–expressing cells were isolated by fluorescence-activated cell sorting resulting in a population expressing a single peak of green fluorescent protein. This population of cells was designated PC-3 Luc and freshly thawed before each experiment.

Animals for *In vivo* Studies

Athymic (R-Foxn1<nu>) nude male mice were obtained from Taconic Farms and maintained under specific pathogen-free conditions. Male mice ages between 4 and 6 weeks were used for the intracardiac challenge model. Purina Rodent Chow 5002 (Ralston Purina) or Harlan Teklad Rodent Diet 8728C and tap water were provided *ad libitum*. The laboratory housing the cages provided a 12-h light cycle and met all Association for Assessment and Accreditation of Laboratory Animal Care specifications. The animals were observed daily to twice daily for mortality and moribundity. All experiments done at Amgen were approved and done in accordance with guidelines set out by the Amgen Animal Use and Care Committee.

Experimental Procedures and Assessments

Intracardiac Model of Bone Metastasis. Four- to 6-week-old male athymic *nu/nu* mice were challenged with 1×10^6 PC-3 Luc cells injected into the left cardiac ventricle. The accuracy of injections was verified by the pattern of bioluminescence. *In vivo* BLI of mice was done with an IVIS 200 imager (Xenogen). Before imaging, mice were given an i.p. injection of D-luciferin and anesthetized with isofluorane. Mice were imaged twice weekly beginning on day 7 after tumor challenge. Dorsal and ventral images of mice were acquired, and images were analyzed using Living Image software (Xenogen). Images were gated for regions of interest that included the whole body, hind limbs, and head area. Animals were monitored weekly for osteolytic disease progression by digital X-ray (Faxitron). Hind limb and head regions correspond to areas with focused bioluminescent signals that progress to develop osteolytic bone lesions.

A preliminary docetaxel (NDC 0075-8001-20; Aventis Pharmaceuticals) dose-ranging study in PC-3 Luc intracardiac-challenged mice with a 14-day preexisting tumor burden compared the following dosages of docetaxel: 10, 20, and 30 mg/kg once weekly. Mice were dosed with two i.p. injections 7 days apart. Treatment of tumor-bearing mice with the initial docetaxel dose resulted in an immediate reduction in the skeletal tumor growth of PC-3 Luc cells as measured by BLI. Treatment with a lower dosage of docetaxel (10 mg/kg weekly) also resulted in an immediate reduction in the growth rate of PC-3 Luc *in vivo* compared with vehicle control and this growth rate reduction was maintained after the second dosage of docetaxel. However, the magnitude and duration of tumor growth suppression was clearly not as complete as that seen with the 20 or 30 mg/kg weekly dosages (data not shown). After the second 20 mg/kg dose of docetaxel, tumor burden declined and reached a nadir ~2 weeks after chemotherapy administration. The increase in bioluminescence observed in the hind limbs after cessation of docetaxel treatment suggested that the chemotherapy did not result in a complete remission.

For combination studies, mice were assigned to the following four groups based on day 10 whole-body bioluminescence, such that each group had an equal distribution of bioluminescence: (*a*) PBS thrice weekly s.c. beginning on day 11 after tumor challenge/saline i.p. on days 11 and 18 after tumor challenge, (*b*) human OPG-Fc 3 mg/kg thrice weekly s.c. beginning on day 11 after tumor

challenge/saline i.p. on days 11 and 18 after tumor challenge, (*c*) PBS thrice weekly s.c. beginning on day 11 after tumor challenge/docetaxel 10 mg/kg bolus injection i.p. on days 11 and 18 after tumor challenge, and (*d*) OPG-Fc 3 mg/kg thrice weekly s.c. beginning on day 11 after tumor challenge plus docetaxel 10 mg/kg bolus injection i.p. on days 11 and 18 after tumor challenge. Animals were either sacrificed at the end of study on day 28 after tumor challenge for histologic evaluation or monitored for time to a weight loss of 20% of initial weight as a surrogate for mortality. Serum samples were collected at the time of necropsy and frozen at −80°C. Serum tartrate-resistant alkaline phosphatase 5b (TRAP-5b) levels were measured by ELISA using MouseTRAP Assay (Immunodiagnostic Systems). Femurs and tibias were carefully separated at the knee joint, cleaned of muscle tissue, fixed in formalin for 48 h, decalcified with a modified 10% formic acid, and processed for paraffin embedding. Each bone was embedded consistently to allow analysis of the entire section of the tibia from ankle to tibial plateau and from the femoral head and third trochanter to the femoral condyle. Tumor area measurements were done on H&E-stained sections of tibias and femurs from each mouse and quantified using Osteo II software (Bioquant) in a blinded fashion by a pathologist; intrabone tumor area was reported as mm^2. Consecutive sections of each metastatic femur and tibia were immunoassayed for TRAP staining, cell proliferation using an antibody against phosphorylated histone H3 (Upstate Cell Signaling), and apoptosis using an antibody against active caspase-3 (Cell Signaling Technology). Immunohistochemistry slides were evaluated in a blinded fashion by a pathologist. The number of cells staining positive was manually counted on the entire intrabone tumor area of the section. Ratios of number of positive cells for phosphorylated histone H3 and active caspase-3 by tumor area were obtained. X-ray lesion areas were calculated using MetaMorph Imaging software (Molecular Devices) on randomized blinded images.

S.c. Tumor Model. Six- to 8-week-old male athymic *nu/nu* mice were injected s.c. with 1×10^6 human PC-3 Luc cells suspended 1:1 in a mixture of Matrigel (BD Biosciences). Tumor dimensions were measured by a digital caliper twice weekly. Tumor volumes were calculated as [length × $(\text{width})^2$ / 2]. Animals were randomized into the following four treatment groups based on day 12 tumor volume measurements: (*a*) PBS thrice weekly s.c. beginning on day 13 after tumor challenge/saline i.p. on days 13 and 20 after tumor challenge, (*b*) human OPG-Fc 3 mg/kg thrice weekly s.c. beginning on day 13 after tumor challenge/saline i.p. on days 13 and 20 after tumor challenge, (*c*) PBS thrice weekly s.c. beginning on day 13 after tumor challenge/docetaxel 10 mg/kg bolus injection i.p. on days 13 and 20 after tumor challenge, and (*d*) OPG-Fc thrice weekly s.c. beginning on day 13 plus docetaxel 10 mg/kg bolus injection i.p. on days 13 and 20 after tumor challenge.

Statistics

Statistical analyses were done using SAS software (SAS Institute). For bioluminescent data, log-transformed data were assessed using a repeated-measures ANOVA model fitted using SAS Proc Mixed to evaluate overall effects of treatment, day, and treatment-by-day interaction. The model was also used to compare individual treatment groups versus the PBS/saline control group at an average level over the entire observation time period. The treatment group comparisons were further conducted at each time point using SAS Proc GLM. The Dunnett's test was applied for the multiple comparisons adjustment in both mixed-effect model and comparisons at individual time points. For histologic measurements, a two-way ANOVA model was fitted using SAS Proc GLM. The Tukey's multiple comparison method was used for comparing individual groups. The comparison of survival time was analyzed with the log-rank test using JMP7 statistical software (SAS Institute).

Results

Optimization of an Experimental Prostate Cancer Bone Metastasis Model

We showed previously that PC-3 prostate tumor growth within the skeleton increased local RANKL levels, which consequently led to significant osteolytic lesions that were effectively blocked by OPG-Fc treatment (21). However, this invasive methodology did not allow for longitudinal measurements and was cumbersome for the analysis of combination treatment effects of OPG-Fc and chemotherapies.

To further understand the effects of drug treatments on prostate tumor growth in the bone, we developed an *in vivo* model in which disease progression can be quantified at skeletal and extraskeletal sites using an optical imaging system. PC-3 cells that had been selected *in vivo* for bone growth were stably transduced with Luc (PC-3 Luc) and injected into the left cardiac ventricle. As early as 3 to 5 days after intracardiac injection, tumor-bearing mice developed a pattern of bioluminescence consistent with tumor metastatic foci in bone, with the highest concentration in hind limbs and mandible (Fig. 1A). The localization of skeletal tumor determined by BLI precisely correlated with radiographic evidence of focal osteolysis (Fig. 1B), with osteolytic lesions first becoming evident on day 14 (data not shown). At day 28, histologic assessment of tissues confirmed that tumor burden was apparent in all of the hind limbs and jaws of all tumor-bearing mice. In addition, histopathologic analysis of soft tissues confirmed that the whole-body BLI signals observed in anatomic locations distinct from the skeleton correlated with small metastatic foci (e.g., minimal tumor was sporadically observed in adrenal glands and lymph nodes; data not shown). Thus, there was minimal extraskeletal metastasis in this model as measured by BLI and histology. Skeletal tumor burden could then be quantified by hind limb BLI, whereas whole-body BLI measurements included both skeletal and the minimal extraskeletal tumor burden.

Before combining anti-RANKL treatment with chemotherapy in this model, we first established the effectiveness

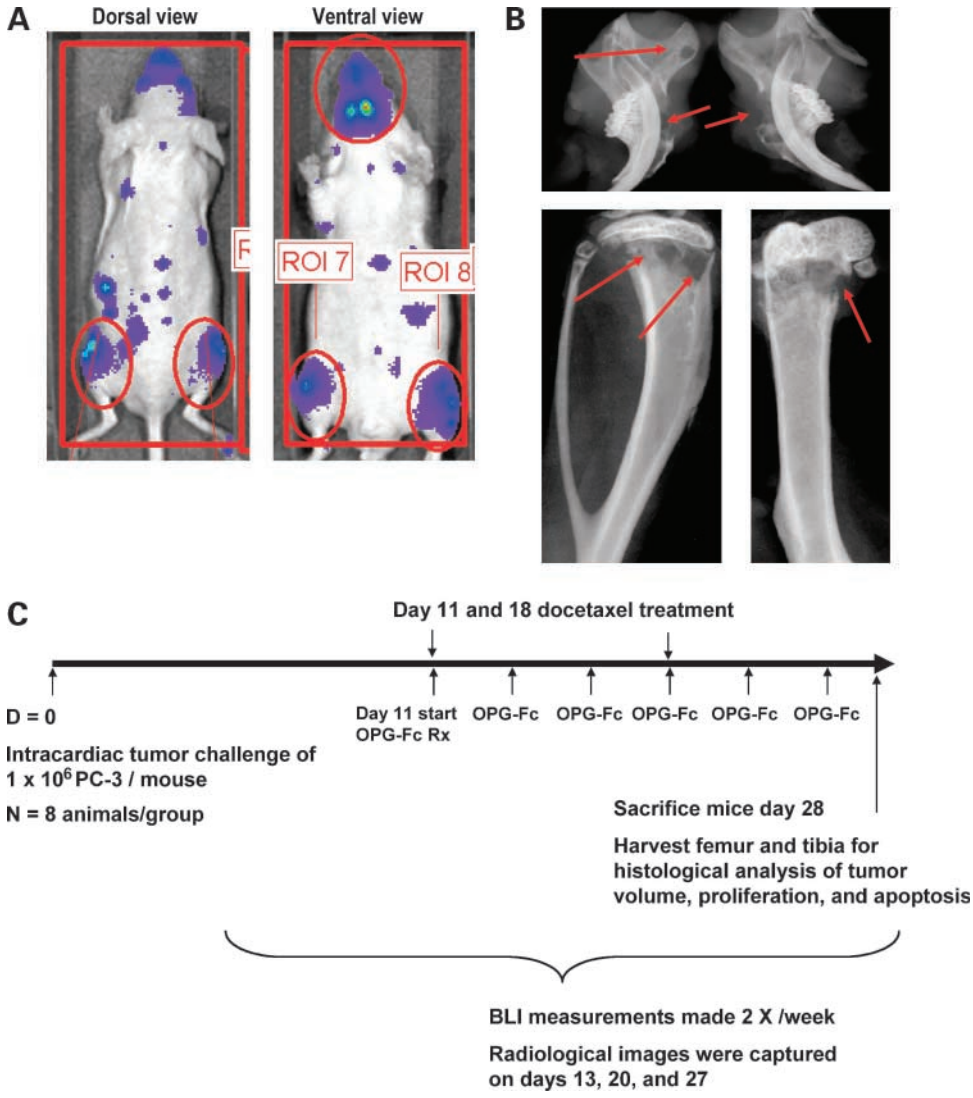

Figure 1. **A** and **B,** bioluminescent and X-ray imaging of PC-3 prostate cancer bone metastases *in vivo*. *In vivo* monitoring of intracardiac-challenged mice was done by BLI. **A,** mice were imaged both ventrally and dorsally for whole-body and specific regions of interest composed of hind limb and mandibular regions. **B,** radiographs confirmed the presence of tumor-induced osteolysis (*red arrows*) that corresponded with BLI signal. **C,** study design: intracardiac model of established bone metastases using PC-3 prostate cancer cells.

of the chemotherapy, docetaxel, as a single agent to reduce skeletal tumor growth. Treatment of mice with established skeletal metastases (day 14) with the initial docetaxel dose (10, 20, or 30 mg/kg weekly) resulted in an immediate reduction in the skeletal (hind limb) and whole-body tumor growth of PC-3 Luc cells as measured by BLI. Using this methodology, we determined that the docetaxel 10 mg/kg dose was suboptimal for reduction of PC-3 Luc skeletal tumor burden over the 28-day time course and therefore would be an appropriate dose to test for the ability of OPG-Fc to enhance chemotherapeutic effects on tumor progression.

OPG-Fc Augmented the *In vivo* Therapeutic Effects of Docetaxel in an Experimental Prostate Cancer Bone Metastasis Model

The schema for treatment schedules is illustrated in Fig. 1C. Treatment of animals with established PC-3 Luc skeletal tumors with 10 mg/kg docetaxel resulted in significant reduction in tumor burden as measured by BLI in all regions evaluated including hind limbs, head, and whole body. The effects of docetaxel were observed as early as 3 days post initiation of therapy culminating with an 80.8% ($P < 0.0001$ versus PBS) reduction in bioluminescence by day 27 post-tumor challenge (Fig. 2). This reduction was consistent between each of the regions evaluated, including hind limbs (Fig. 2A), whole body (Fig. 2B), and head (data not shown). Treatment with OPG-Fc alone had a small effect on tumor burden as measured by BLI, resulting in a 20.9% decrease in hind limb tumor growth and a 16.0% decrease in whole-body tumor growth at day 27 (Fig. 2A and B). This reduction did not reach statistical significance. However, by combining OPG-Fc with docetaxel, the reduction of hind limb tumor burden (96.7% inhibition versus PBS) was significantly greater than docetaxel alone ($P = 0.0026$; Fig. 2A). The inhibitory effect of combining OPG-Fc with docetaxel was also significantly

greater than docetaxel alone at other bony anatomic sites (head; $P = 0.0008$; data not shown) as well as the whole body ($P = 0.0005$; Fig. 2B). The percent reductions in hind limb and whole-body BLI by either treatment alone or in combination are summarized in the summary tables below Fig. 2A and B, respectively. The relatively large contribution of skeletal tumor metastasis relative to whole-body tumor burden is reflected by reductions in whole-body BLI by both OPG-Fc and docetaxel (alone and in combination) treatments. This latter observation also indicates that treatment with either agent does not shift tumor burden from skeletal sites to other nonskeletal sites.

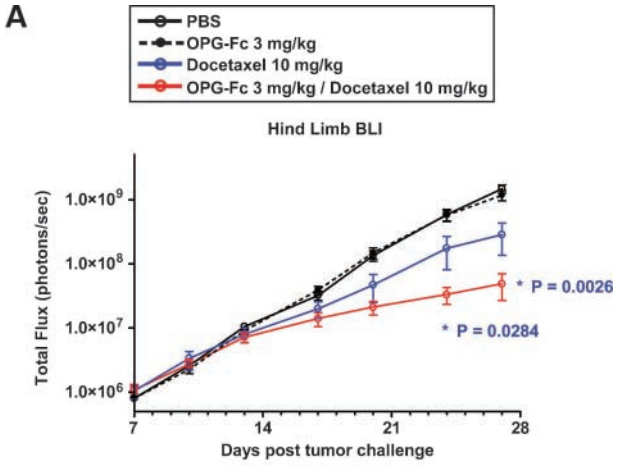

Hind Limb Bioluminescence	% Reduction Day 24	% Reduction Day 27
PBS	0.00%	0.00%
OPG-Fc 3 mg/kg	2.86%	20.87%
Docetaxel 10 mg/kg	70.27%[a]	80.77%[a]
OPG-Fc 3 mg/kg + Docetaxel10 mg/kg	94.39%[a,b]	96.73%[a,c]

[a]$P < 0.0001$ vs PBS; [b]$P = 0.0284$ vs Docetaxel; [c]$P = 0.0026$ vs Docetaxel

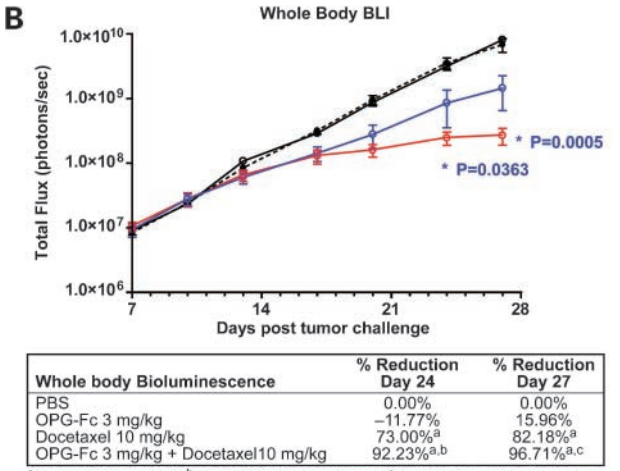

Whole body Bioluminescence	% Reduction Day 24	% Reduction Day 27
PBS	0.00%	0.00%
OPG-Fc 3 mg/kg	−11.77%	15.96%
Docetaxel 10 mg/kg	73.00%[a]	82.18%[a]
OPG-Fc 3 mg/kg + Docetaxel10 mg/kg	92.23%[a,b]	96.71%[a,c]

[a]$P < 0.0001$ vs PBS; [b]$P = 0.0363$ vs Docetaxel; [c]$P = 0.0005$ vs Docetaxel

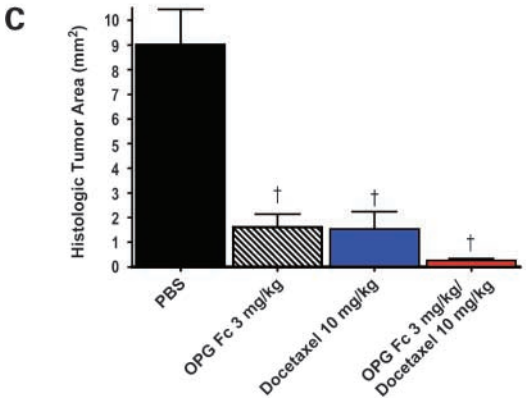

Direct histologic analysis of the skeletal tumor burden area showed that all treatment groups experienced significant reductions in the hind limbs of challenged mice relative to PBS control (Fig. 2C). OPG-Fc and docetaxel as single agents reduced the histologic tumor burden within the bone by 82% ($P < 0.0001$ versus PBS) and by 83% ($P = 0.0001$ versus PBS), respectively. When treatments were combined, the antitumor effect was enhanced to 97.5% reduction compared with the PBS control group ($P < 0.0001$ versus PBS).

RANKL Inhibition Suppressed Tumor Growth by Decreasing Tumor Cell Proliferation and Increasing Tumor Cell Apoptosis in Bone

To assess treatment effects on tumor cell growth and viability, we used immunohistochemistry to evaluate markers of apoptosis (active caspase-3) and proliferation (phosphorylated histone H3). Tumor cells in bones that had been treated with either OPG-Fc (3 mg/kg) or docetaxel (10 mg/kg) as single agents showed a significantly higher degree of apoptosis (Fig. 3A and B; 5-fold increase with OPG-Fc, $P = 0.0086$ versus PBS; 6-fold increase with docetaxel, $P = 0.0097$ versus PBS) compared with PBS control. Furthermore, the increased tumor cell apoptosis was most pronounced (11-fold increase, $P = 0.0006$ versus PBS) in the OPG-Fc/docetaxel combination group, although this latter observation was not significantly different from either monotherapy alone ($P = 0.07$). Reductions in tumor cell proliferation in animals treated with OPG-Fc plus docetaxel were also observed (Fig. 3A), although these differences were not statistically significant (Fig. 3C).

Treatment Effects on Tumor-Induced Osteolysis

PC-3 tumor-induced osteolysis was evident by radiographic analysis at 14 days and progressed significantly with time (ref. 21; data not shown). Treatment with OPG-Fc completely prevented the development of osteolytic bone lesions whether as a single agent or combined with docetaxel (Fig. 4A and C). The prevention of osteolysis in

Figure 2. OPG-Fc inhibited progression of established skeletal tumors and enhanced the effects of docetaxel. Bioluminescent images were captured twice weekly beginning on day 7 post-tumor challenge. OPG-Fc and/or docetaxel treatment began on day 11 post-tumor challenge. Data for hind limb (**A**) and whole-body (**B**) regions are combined values from dorsal and ventral images. Mean ± SE for each group ($n = 8$ per group). The bioluminescent signal from all mice treated with docetaxel was significantly reduced relative to the PBS group from day 13 (whole-body BLI) or day 20 (hind limb BLI) until the termination of the study. *P* values are given for the OPG-Fc/docetaxel group when significantly different than docetaxel alone. **C,** OPG-Fc, alone or in combination with docetaxel, significantly reduced histologic intrabone tumor area. Mean tumor area ± SE. †, OPG-Fc: $P < 0.0001$ versus PBS; docetaxel: $P = 0.0001$ versus PBS; OPG-Fc/docetaxel: $P < 0.0001$ versus PBS.

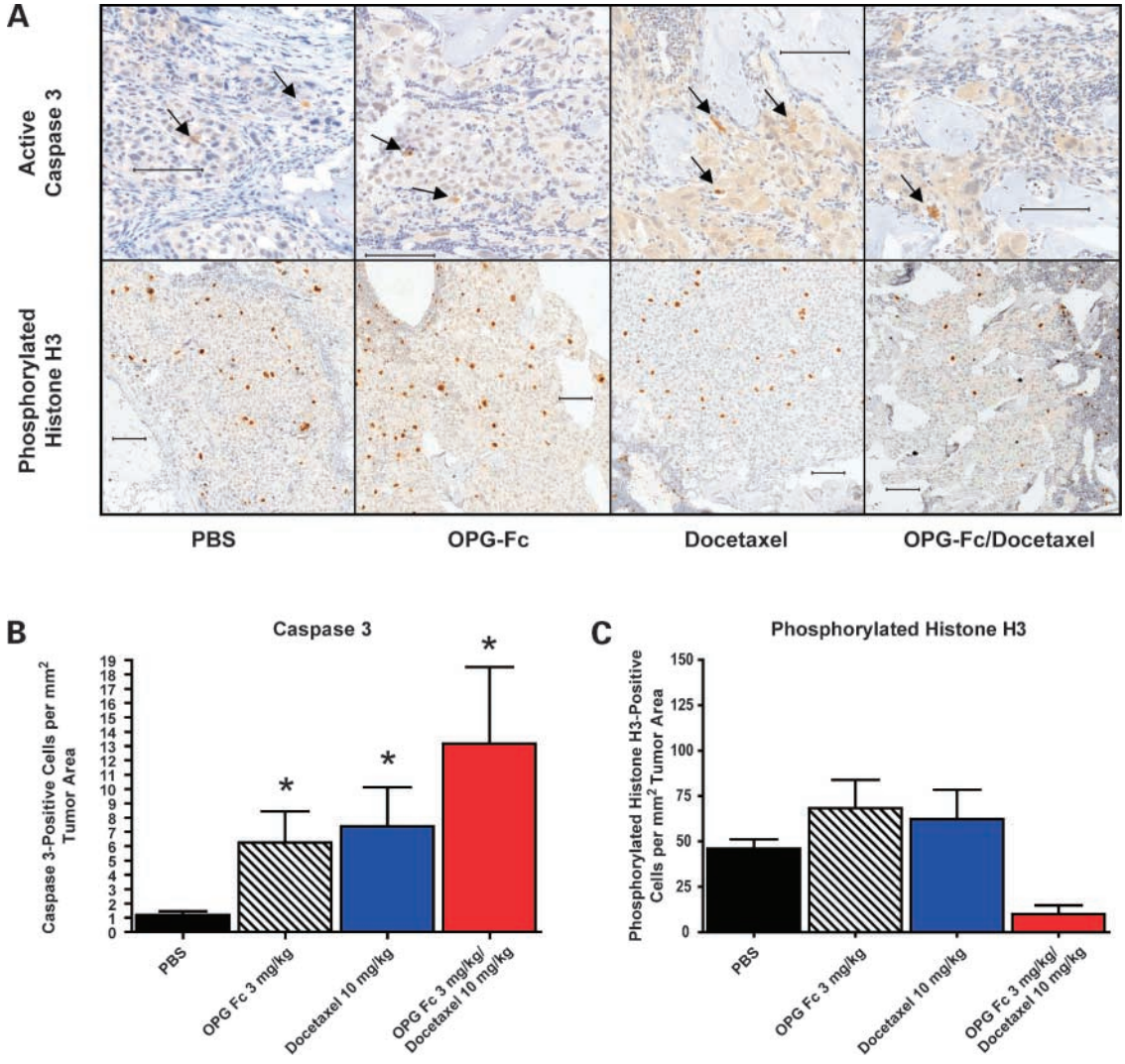

Figure 3. OPG-Fc increased tumor cell apoptosis in PC-3 bone metastases. OPG-Fc and/or docetaxel treatment began on day 11 post-tumor challenge. **A,** sections of metastatic femur and tibia that were immunoassayed for tumor cell apoptosis by probing with antibodies specific to active caspase-3 or for tumor cell proliferation by probing with antibodies specific to phosphorylated histone H3 (*brown*) and counterstained with H&E ($n = 8$ per group). Histologic images were captured from ×20 scans using an Aperio T2 Scanscope (Aperio) with an Olympus ×20/0.75 UplanSApo objective. Bar, 100 μm. *Arrows,* active caspase-3-positive cells. **B,** ratios of the number of cells positive for caspase-3 staining by tumor area ± SE. *, OPG-Fc: $P = 0.0086$ versus PBS; docetaxel: $P = 0.0097$ versus PBS and OPG-Fc/docetaxel: $P = 0.0006$ versus PBS). **C,** ratios of number of positive cells for phosphorylated histone H3 staining by tumor area ± SE.

those groups treated with OPG-Fc was achieved by reductions in osteoclast function as measured by the absence of TRAP5b-positive osteoclasts within the bone both at the tumor/bone interface and at regions on normal bone (TRAP5b histology; Fig. 4C). Reductions in serum levels of TRAP5b (Fig. 4B) confirmed the ability of OPG-Fc to reduce systemic osteoclast function either when used alone or with docetaxel. Docetaxel treatment led to a minimal reduction in tumor-associated osteoclasts (TRAP5b histology; Fig. 4C) and a reduction in osteolytic lesions in this group (Fig. 4A), although this effect was incomplete as radiographically evident lesions were still observed in the docetaxel treatment group (Fig. 4C). The reduction in osteoclasts by docetaxel treatment was not due to a direct effect on osteoclasts as indicated by normal levels of serum TRAP5b in this group (Fig. 4B). Instead, docetaxel likely reduced tumor-induced osteoclastogenesis indirectly as a result of reduced tumor burden at the skeleton as shown above in Fig. 2.

RANKL Inhibition Significantly Improved Survival as a Monotherapy or in Combination with Docetaxel

We next investigated whether the reduction in skeletal PC-3 Luc tumor progression by these treatments would affect the survival of tumor-bearing mice. Kaplan-Meier survival curves after OPG-Fc treatment are presented in Fig. 5. Although the median survival time for PBS-treated

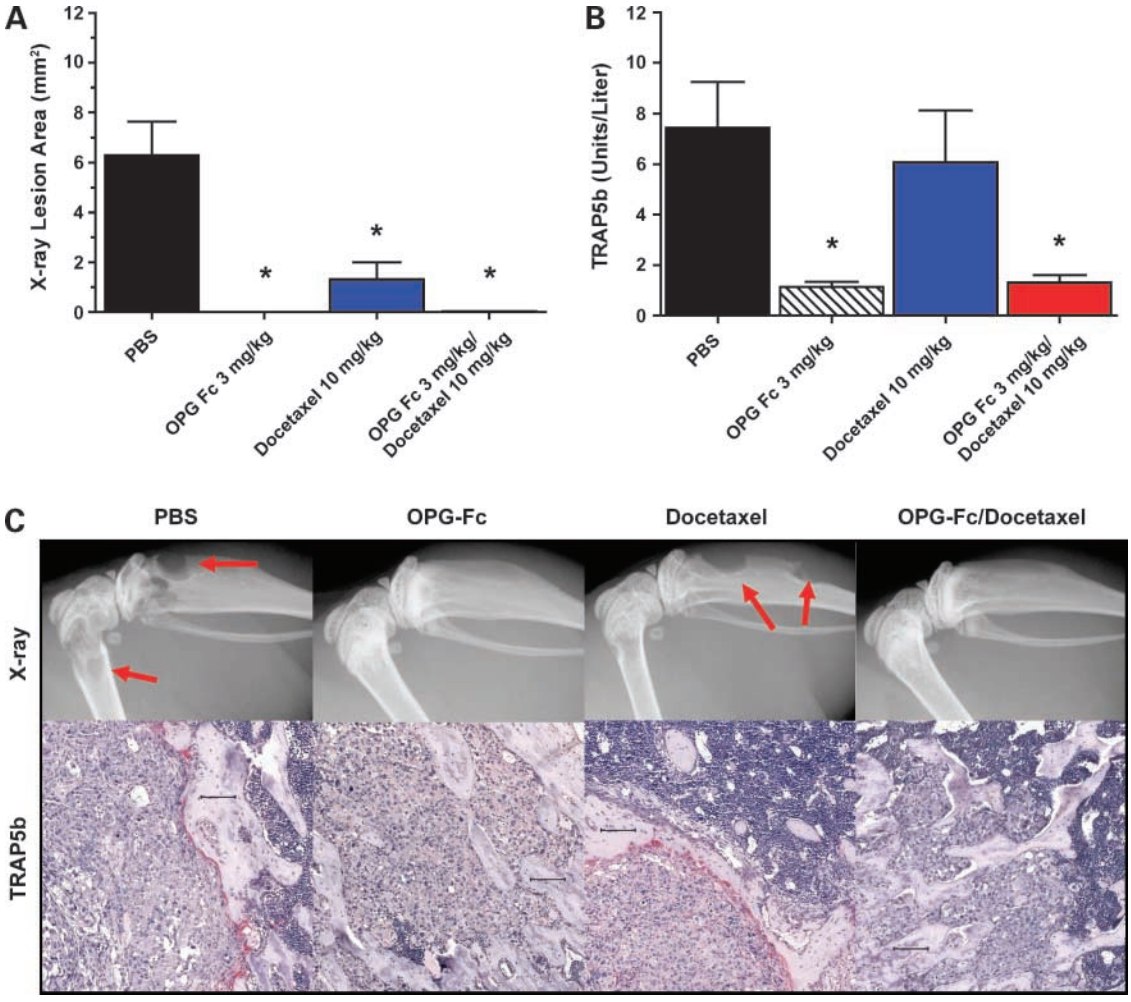

Figure 4. OPG-Fc and docetaxel treatments inhibited tumor-induced osteolysis. OPG-Fc and/or docetaxel treatment began on day 11 post-tumor challenge. **A,** X-ray lesion area was determined from femurs and tibia at day 27 post-tumor challenge. Mean lesion area/mouse ± SE (n = 8 per group). **B,** serum samples were collected at the time of necropsy and frozen at −80°C. Serum TRAP5b levels were measured by ELISA using MouseTRAP Assay (Immunodiagnostic Systems). Mean concentration ± SD (n = 8 per group). *, $P < 0.001$ versus PBS by one-way ANOVA with Bonferroni's post-test. **C,** representative radiographs and TRAP5-stained histologic images showing no osteoclasts in the OPG-Fc and OPG-Fc/docetaxel treatment groups. *Red arrows,* osteolytic lesions in the PBS and docetaxel groups. Histologic images were captured from ×20 scans using an Aperio T2 Scanscope (Aperio) with an Olympus ×20/0.75 UplanSApo objective. Bar, 100 μm.

PC-3 Luc tumor-bearing animals was 30 days, OPG-Fc treatment led to a 23% increase in survival (P = 0.0003 versus PBS) to a median of 37 days. Treatment of tumor-bearing mice with 10 mg/kg docetaxel increased survival to 39 days, whereas the combination of OPG-Fc with docetaxel prolonged survival by 16.7% (median survival, 45.5 days), which was significantly greater compared with docetaxel alone (P = 0.0385).

RANKL Inhibition Had No Effect on S.c. PC-3 Luc Tumors

We implanted PC-3 Luc tumors s.c. in the flanks of mice. Docetaxel 10 mg/kg treatment resulted in a significant reduction in tumor progression, whereas OPG-Fc treatment (either alone or in combination with docetaxel) had no effect on the growth of PC-3 Luc tumor cells in this nonosseous setting (Fig. 6).

Discussion

Bone metastases from prostate cancer and other malignancies are associated with severe skeletal complications, collectively termed skeletal-related events, which are a major clinical problem. Although prostate cancer bone metastases are typically characterized as osteoblastic according to radiographic appearance, there is also a prominent osteolytic component that contributes to increased bone destruction and subsequently to the observed skeletal-related events (11, 22–24).

RANKL, RANK, and OPG are key mediators of osteoclastogenesis and bone resorption that likely contribute to the underlying pathogenesis of prostate cancer bone metastases. RANKL, a protein expressed by osteoblasts, is essential for osteoclastogenesis (25). Previous studies in several prostate cancer mouse models have shown that

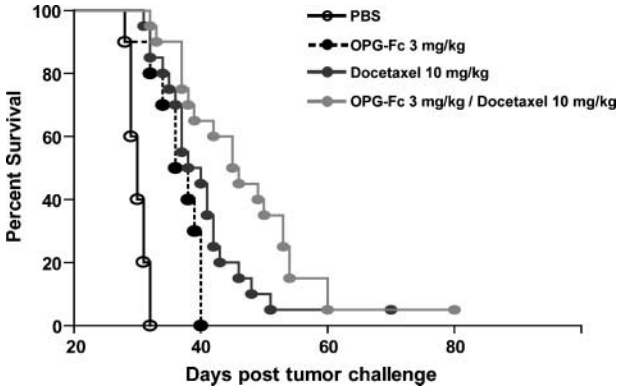

Figure 5. OPG-Fc, alone or in combination with docetaxel, increased survival of PC-3-challenged mice. OPG-Fc and/or docetaxel treatment began on day 11 post-tumor challenge. Mice with established bone metastases on treatment were monitored until they became moribund and experienced hind limb paralysis or 20% weight loss (operative definition of ''survival''), at which point the mice were euthanized. The Kaplan-Meier plot shows significant improvement in survival with OPG-Fc alone or in combination with docetaxel. The OPG-Fc group showed a 23% increase in survival (time to moribund state) compared with the PBS control ($P = 0.0003$, $n = 10$ per group). Median survival times were 30 d for PBS and 37 d for OPG-Fc. OPG plus docetaxel increased survival by 16.7% compared with docetaxel alone ($P = 0.0385$, $n = 20$ per group). Median survival times were 39 d for docetaxel and 45.5 d for OPG-Fc plus docetaxel.

inhibiting RANKL with OPG-Fc or RANK-Fc prevented the development of bone lesions and the progression of prostate tumor in the bone (reviewed in ref. 26). Similar results were observed in models of lytic disease (21, 27), ''mixed'' osteolytic/osteoblastic lesions (16, 28), and purely osteoblastic lesions (27, 29). It will be important to test whether the combination effect of RANKL inhibition plus docetaxel on skeletal tumor burden observed with this osteolytic prostate cancer model will extend to mixed or osteoblastic bone lesions.

PC-3 prostate cancer cells have been shown to produce factors such as interleukin-1 and tumor necrosis factor-α(30), which both have pleiotropic actions on osteoclast functions and activation. The production of these factors correlated with the osteolytic phenotype of PC-3 tumors (30) and may contribute to the excessive osteolysis observed. Tumor necrosis factor-α and interleukin-1 have been shown to increase RANKL mRNA within osteoblasts and/or stromal cells (31, 32) and can synergize with permissive levels of RANKL to increase osteoclastogenesis (33) and increase circulating osteoclast precursors (34). In this study, osteoclastogenesis was completely suppressed after OPG-Fc treatment, suggesting that tumor cell production of interleukin-1 or tumor necrosis factor-α (or any other factor) did not circumvent the RANK/RANKL pathway in osteoclast formation *in vivo*.

The progression of the established skeletal tumor is supported by the mutual interplay between locally increased osteoclastic activity and tumor cell proliferation (the ''vicious cycle;'' ref. 35), which may also facilitate earlier steps in skeletal tumor establishment and development (5). Treatment of PC-3 tumor-bearing animals with OPG-Fc had no obvious effects on the production of other host cytokines and factors (data not shown). Therefore, reduction in tumor progression observed after RANKL inhibition is likely the consequence of interrupting the ''vicious cycle,'' which leads to a reduction in local concentrations of bone-derived factors as a result of lower osteoclastic bone resorption.

Importantly, bone-derived growth factors such as insulin-like growth factor-1, transforming growth factor-β, basic fibroblast growth factor, interleukin-6, and parathyroid hormone-releasing protein (36) have been shown to inhibit chemotherapy-induced tumor cell apoptosis *in vitro* and may contribute to resistance to chemotherapies in metastatic prostate cancer (37). Taxanes have shown therapeutic activity; despite an improvement in overall survival, cancer progression still occurs in nearly all patients receiving this treatment (19, 20). Because 90% of these patients have bone metastases, we hypothesized that combining bone-targeted agents (OPG-Fc) with an antineoplastic agent (docetaxel) may provide an additive benefit in suppressing tumor growth by targeting different pathways. This observation was unique to the skeletal microenvironment, as OPG-Fc had no effect on a s.c. PC-3 tumor growth either alone or in combination with docetaxel, which suggests that the mechanism by which RANKL inhibition enhances the chemotherapeutic effects of docetaxel is indirect, via osteoclast inhibition. Further support for this hypothesis is the observation that treatment of PC-3 cells with OPG-Fc *in vitro* had no detectable effects on cell proliferation or survival (data not shown), yet the reduction in tumor growth observed in the bone after OPG-Fc treatment was correlated with a trend toward lower tumor cell proliferation and a significant increase in tumor cell apoptosis.

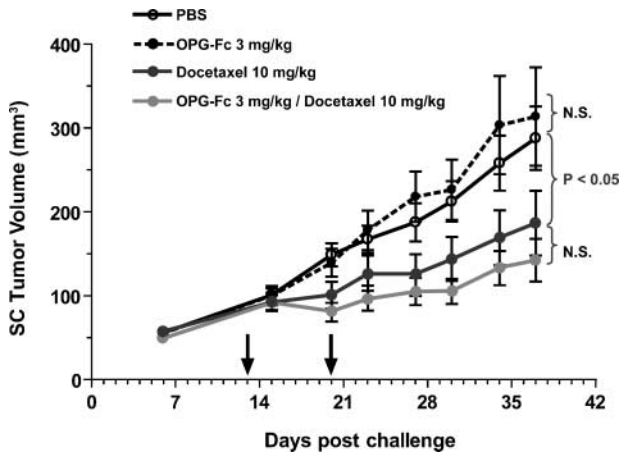

Figure 6. OPG-Fc treatment did not alter the growth of s.c. PC-3 tumor cells *in vivo*. OPG-Fc and/or docetaxel treatment began on day 13 post-tumor challenge. Treatment of s.c. implanted PC-3 Luc tumor cells (1×10^6 per 50 μL injection) with docetaxel significantly reduced tumor growth. OPG-Fc alone did not alter s.c. tumor progression. Tumor volume ± SE ($n = 13$ per group). Docetaxel: $P < 0.05$ versus PBS; OPG-Fc: not significant (*N.S.*) versus PBS.

Although the ability of RANKL inhibition to enhance docetaxel effects on established skeletal tumor burden were evident at day 27 in this model, additional experiments are necessary to determine the optimal sequence and timing of this combination therapy.

There was a clear and statistically significant reduction by OPG-Fc treatment (as a monotherapy) on the intrabone tumor area (as measured by histology); however, the hind limb tumor burden as measured by BLI was not significantly reduced (20.87% reduction at day 27). This apparent discrepancy can be explained by the different aspects of tumor growth analyzed by these two distinct analytical approaches. PC-3 tumors are highly osteolytic producing round holes through the tibia and femur cortices in the PBS-treated control animals and will ultimately break through the cortex and grow in the soft tissue surrounding the bone. The BLI imaging of the hind limbs include both tumor growth within the medullary cavity and extraskeletal growth, whereas the histologic analysis only addresses intrabone tumor area. The effects of docetaxel are independent of tumor localization and therefore can reduce both intrabone and extramedullary tumor growth, whereas OPG-Fc effects were limited to skeletal site. Therefore, the effects of OPG-Fc (when used alone) on skeletal tumor burden are more clearly evident in the histologic analysis, whereas the ability of OPG-Fc to enhance docetaxel can be observed by BLI.

The degree of bone resorption in prostate cancer patients with bone metastases influences the course of disease as serum markers of urinary *N*-telopeptide type I collagen has been shown to be predictive of skeletal-related events, bone disease progression, and death (7, 12). This study shows a significant effect of RANKL inhibition (either as a monotherapy or in combination with docetaxel) on survival of animals bearing PC-3 tumor-induced bone lesions. The therapeutic effect of the monotherapy and combination treatments was correlated with the inhibition of osteoclast function and induction of tumor cell apoptosis. Histologic analysis showed that both OPG-Fc and docetaxel had significant effects in reducing skeletal tumor burden; however, the survival benefit was not entirely predicted, because residual tumor burden remained in all treatment groups. Given that the majority of PC-3 tumor burden resided within the skeleton after 28 days postintracardiac injection, the prolongation of animal survival in the OPG-Fc-treated group suggests that the skeletal prostate tumor burden has an incremental and significant effect on survival. Although it is unclear if the modest survival benefit shown in this study will provide any clinical benefit, a similar increase in survival of tumor-bearing animals after RANKL inhibition has been observed in a model of multiple myeloma (38) and breast cancer bone metastasis (39).

In conclusion, our data show that RANKL inhibition not only inhibited pathologic osteolysis induced by human prostate carcinoma PC-3 cells in animals with established tumors but also enhanced the effect of docetaxel to reduce skeletal tumor burden and prolong survival. The results of this study support further research on the use of chemotherapy in combination with RANKL inhibition to suppress tumor-induced osteolysis and inhibit the growth of skeletal tumors.

Disclosure of Potential Conflicts of Interest

All authors are employees of Amgen and have received stock/stock options from Amgen.

Acknowledgments

We thank Guang Chen for discussions of the statistical analyses of data, Mark Tometsko and Michelle Chaisson-Blake for helpful discussions, and Ting Chang, Ph.D., for expert editorial support.

References

1. Bubendorf L, Schopfer A, Wagner U, et al. Metastatic patterns of prostate cancer: an autopsy study of 1,589 patients. Hum Pathol 2000; 31:578 – 83.

2. Coleman RE. Clinical features of metastatic bone disease and risk of skeletal morbidity. Clin Cancer Res 2006;12:6243 – 9s.

3. Roudier MP, Vesselle H, True LD, et al. Bone histology at autopsy and matched bone scintigraphy findings in patients with hormone refractory prostate cancer: the effect of bisphosphonate therapy on bone scintigraphy results. Clin Exp Metastasis 2003;20:171 – 80.

4. Sabbatini P, Larson SM, Kremer A, et al. Prognostic significance of extent of disease in bone in patients with androgen-independent prostate cancer. J Clin Oncol 1999;17:948 – 57.

5. Roodman GD. Mechanisms of bone metastasis. N Engl J Med 2004; 350:1655 – 64.

6. Charhon SA, Chapuy MC, Delvin EE, Valentin-Opran A, Edouard CM, Meunier PJ. Histomorphometric analysis of sclerotic bone metastases from prostatic carcinoma special reference to osteomalacia. Cancer 1983; 51:918 – 24.

7. Coleman RE, Major P, Lipton A, et al. Predictive value of bone resorption and formation markers in cancer patients with bone metastases receiving the bisphosphonate zoledronic acid. J Clin Oncol 2005;23: 4925 – 35.

8. Stewart AF, Vignery A, Silverglate A, et al. Quantitative bone histomorphometry in humoral hypercalcemia of malignancy: uncoupling of bone cell activity. J Clin Endocrinol Metab 1982;55:219 – 27.

9. Urwin GH, Percival RC, Harris S, Beneton MN, Williams JL, Kanis JA. Generalised increase in bone resorption in carcinoma of the prostate. Br J Urol 1985;57:721 – 3.

10. Chirgwin JM, Guise TA. Molecular mechanisms of tumor-bone interactions in osteolytic metastases. Crit Rev Eukaryot Gene Expr 2000;10:159 – 78.

11. Demers LM, Costa L, Lipton A. Biochemical markers and skeletal metastases. Cancer 2000;88:2919 – 26.

12. Brown JE, Cook RJ, Major P, et al. Bone turnover markers as predictors of skeletal complications in prostate cancer, lung cancer, and other solid tumors. J Natl Cancer Inst 2005;97:59 – 69.

13. Boyle WJ, Simonet WS, Lacey DL. Osteoclast differentiation and activation. Nature 2003;423:337 – 42.

14. Morony S, Capparelli C, Sarosi I, Lacey DL, Dunstan CR, Kostenuik PJ. Osteoprotegerin inhibits osteolysis and decreases skeletal tumor burden in syngeneic and nude mouse models of experimental bone metastasis. Cancer Res 2001;61:4432 – 6.

15. Quinn JE, Brown LG, Zhang J, Keller ET, Vessella RL, Corey E. Comparison of Fc-osteoprotegerin and zoledronic acid activities suggests that zoledronic acid inhibits prostate cancer in bone by indirect mechanisms. Prostate Cancer Prostatic Dis 2005;8:253 – 9.

16. Zhang J, Dai J, Qi Y, et al. Osteoprotegerin inhibits prostate cancer-induced osteoclastogenesis and prevents prostate tumor growth in the bone. J Clin Invest 2001;107:1235 – 44.

17. Mundy GR, Yoneda T, Hiraga T. Preclinical studies with zoledronic acid and other bisphosphonates: impact on the bone microenvironment. Semin Oncol 2001;28:35 – 44.

18. Chay CH, Cooper CC, Hellerstedt BA, Pienta KJ. Antimetastatic drugs in prostate cancer. Clin Prostate Cancer 2002;1:14 – 9.

19. Petrylak DP, Tangen CM, Hussain MH, et al. Docetaxel and estramustine compared with mitoxantrone and prednisone for advanced refractory prostate cancer. N Engl J Med 2004;351:1513 – 20.

20. Tannock IF, de Wit R, Berry WR, et al. Docetaxel plus prednisone or mitoxantrone plus prednisone for advanced prostate cancer. N Engl J Med 2004;351:1502 – 12.

21. Armstrong AP, Miller RE, Jones JC, Zhang J, Keller ET, Dougall WC. RANKL acts directly on RANK-expressing prostate tumor cells and mediates migration and expression of tumor metastasis genes. Prostate 2008;68:92 – 104.

22. Clarke NW, McClure J, George NJ. Morphometric evidence for bone resorption and replacement in prostate cancer. Br J Urol 1991;68:74 – 80.

23. Roudier MP, True LD, Higano CS, et al. Phenotypic heterogeneity of end-stage prostate carcinoma metastatic to bone. Hum Pathol 2003;34: 646 – 53.

24. Vessella RL, Corey E. Targeting factors involved in bone remodeling as treatment strategies in prostate cancer bone metastasis. Clin Cancer Res 2006;12:6285 – 90s.

25. Lacey DL, Timms E, Tan HL, et al. Osteoprotegerin ligand is a cytokine that regulates osteoclast differentiation and activation. Cell 1998;93: 165 – 76.

26. Dougall WC, Chaisson M. The RANK/RANKL/OPG triad in cancer-induced bone diseases. Cancer Metastasis Rev 2006;25:541 – 9.

27. Whang PG, Schwarz EM, Gamradt SC, Dougall WC, Lieberman JR. The effects of RANK blockade and osteoclast depletion in a model of pure osteoblastic prostate cancer metastasis in bone. J Orthop Res 2005;23: 1475 – 83.

28. Yonou H, Kanomata N, Goya M, et al. Osteoprotegerin/osteoclastogenesis inhibitory factor decreases human prostate cancer burden in human adult bone implanted into nonobese diabetic/severe combined immunodeficient mice. Cancer Res 2003;63:2096 – 102.

29. Zhang J, Dai J, Yao Z, Lu Y, Dougall W, Keller ET. Soluble receptor activator of nuclear factor κB Fc diminishes prostate cancer progression in bone. Cancer Res 2003;63:7883 – 90.

30. Lee Y, Schwarz E, Davies M, et al. Differences in the cytokine profiles associated with prostate cancer cell induced osteoblastic and osteolytic lesions in bone. J Orthop Res 2003;21:62 – 72.

31. Hofbauer LC, Lacey DL, Dunstan CR, Spelsberg TC, Riggs BL, Khosla S. Interleukin-1beta and tumor necrosis factor-α, but not interleukin-6, stimulate osteoprotegerin ligand gene expression in human osteoblastic cells. Bone 1999;25:255 – 9.

32. Horwood NJ, Elliott J, Martin TJ, Gillespie MT. Osteotropic agents regulate the expression of osteoclast differentiation factor and osteoprotegerin in osteoblastic stromal cells. Endocrinology 1998;139: 4743 – 6.

33. Lam J, Takeshita S, Barker JE, Kanagawa O, Ross FP, Teitelbaum SL. TNF-α induces osteoclastogenesis by direct stimulation of macrophages exposed to permissive levels of RANK ligand. J Clin Invest 2000;106: 1481 – 8.

34. Yao Z, Li P, Zhang Q, et al. Tumor necrosis factor-α increases circulating osteoclast precursor numbers by promoting their proliferation and differentiation in the bone marrow through up-regulation of c-Fms expression. J Biol Chem 2006;281:11846 – 55.

35. Guise TA, Mohammad KS, Clines G, et al. Basic mechanisms responsible for osteolytic and osteoblastic bone metastases. Clin Cancer Res 2006;12:6213 – 6s.

36. Koutsilieris M, Mitsiades C, Sourla A. Insulin-like growth factor I and urokinase-type plasminogen activator bioregulation system as a survival mechanism of prostate cancer cells in osteoblastic metastases: development of anti-survival factor therapy for hormone-refractory prostate cancer. Mol Med 2000;6:251 – 67.

37. Reyes-Moreno C, Sourla A, Choki I, Doillon C, Koutsilieris M. Osteoblast-derived survival factors protect PC-3 human prostate cancer cells from Adriamycin apoptosis. Urology 1998;52:341 – 7.

38. Vanderkerken K, De Leenheer E, Shipman C, et al. Recombinant osteoprotegerin decreases tumor burden and increases survival in a murine model of multiple myeloma. Cancer Res 2003;63:287 – 9.

39. Canon J, Roudier M, Bryant R, Radinsky R, Dougall W. Inhibition of RANKL blocks skeletal tumor progression and improves survival in a mouse model of breast cancer bone metastasis. Clin Exp Metastasis 2008; 25:119 – 29.